



ORIGINAL ARTICLE

Performance of F.S.G. Iridology in detecting all diseases, vitamins, and trace mineral in human body within one minute

Rana Cheikh Ousman¹, Mouhamad Tamer Zakor²

¹Assistant Professor, Frequensky Global Society, Department research and development, France

²Professor, Frequensky Global Clinic, Department Alternative Medicine, Kuala Lumpur, Malaysia

Article Information

Received: 27 Sep 2021
Revised: 5 Oct 2021
Accepted: 7 Oct 2021
Available online: 12 Oct 2021

Keywords:

Iridology;
F.S.G.;
Frequensky;
Vitamin;
Diseases;
Mineral.

Abstract

One of the most significant responsibilities of the first step is to predict diseases at an earlier stage and lower long-term treatment costs. Iridology is another option for diagnosing using iris features. With the help of an image processing concept, this research examines the powerful of F.S.G. iridology tool. F.S.G. Iridology is a revolution in iridology science because it is the first time we have been able to develop an iridology device capable of diagnosing and detecting the health status of several body organs in the same times, including Kidney, Adrenal glands, Gallbladder, Liver, Mammary glands, Heart, Bronchi, Lungs, Ears, Hypothalamus, Brain, Nose, Throat, Thyroid gland, Spleen, Oesophagus, Pancreas, Duodenum, Small intestine, Colon, Stomach, Spine, Uterus, Ovaries, Prostate, Testicles, as well as determining trace elements rate (fluorine, chromium, copper, manganese, iodine, iron, and selenium) and some vitamins such as B1, C, E, K. All these diagnoses take only one minute, and they are 100 percent accurate. This avoids some diseases that necessitate the quickest diagnosis possible to avoid a dangerous consequence, accurate, inexpensive, and quick diagnosis, that can save many lives from certain death. Furthermore, by utilizing computer vision on iridology to characterize abnormalities in iris features, F.S.G's diagnosis is cost-effective, robust, reliable, non-contact, non-radioactive, and convenient. ©2021 ijrei.com. All rights reserved

1. Introduction

Human disease diagnosis, whether by blood tests, urine analysis, radiography, or echography, is a difficult, expensive, and time-consuming process [1]. To avoid a dangerous outcome, some disorders require the quickest diagnosis possible. Many lives can be saved if accurate, low-cost, and quick diagnosis is available.

Iridology is the art and science of disclosing and diagnosing disease and inflammation in the human body. It's a quick, painless, and non-invasive method to determine the health of each organ. As eyes are like a geographic map of the body,

diseases are mentioned as marks on the fragment of the iris that is responsible for a specific area of the body.

Iridologists have traditionally used images of a subject's irises to diagnose a malady. This method requires the use of a camera for authorization and authentication of each iris displayed. Throughout history, human eyes have been described as "windows to the soul" The eyes are now recognized as mirrors for the human body's health thanks to the emergence of iris-based studies [2]. Fibrous sheaths of the optic nerves connect the eyes to the Dura mater of the brain, and the iris of the eye is directly linked with a sympathetic nervous system and spinal cord. [3] figure 1.

Corresponding author: Mouhamad Tamer Zakor

Email Address: frq@frequensky.com

<https://doi.org/10.36037/IJREI.2021.5604>

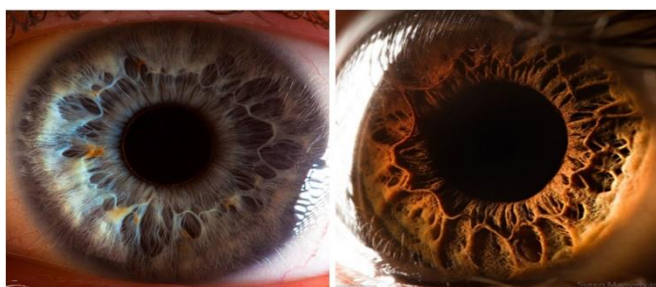


Figure 1: The fibrous structure of the anterior border layer and stroma [3] is seen in this ultra-close-up picture of an eye

According to iridologists, when any change occurs inside the body that is not related to normal activities, a mark or point appears in the iris. This mark or point denotes a change in a certain organ or system of the body [3]. These iris abnormalities aid in the diagnosis of a certain disease. Iridology charts and iris images are used to diagnose ailments such as diabetes, hypertension, and diseases of the liver, digestive system, and skin. For the diagnosis of various diseases, in-vivo, ex-vivo, in-vitro, and many other microbiological and pathologic procedures are used. All these methods necessitate sterile labs, high-tech, pricey equipment, and brutally drained human body samples.

It takes a lot of expertise, experience, and a long time to evaluate the picture of iris changes perfectly and completely. Merging an innovative technique with modern digital technology developments significantly reduces patient examination time, enhances diagnosis accuracy, and clarifies the diagnosis procedure [4]. Iris investigation revealed the eyes' variance and exclusiveness, starting with the supposition that they are all possible alike. For each eye, all iris recognition and process parameters will be used separately. Iridologists use this information in their tests, and a diagnosis is only accurate and complete after both eyes have been realized.

Many researchers have suggested the technique of iris assessment, whether by eye color. Irises come in a variety of colors, ranging from dark brown to bright blue. The external appearance of the eye is characterized by three colors (brown, yellow, and grey) [5]. All of the iris color variations can be linked back to those color combinations (see Fig 2). The procedure for determining the basic iris color is straightforward. All of the predominant colored iris regions should be recognized, and the color of each should be obtained.



Figure 2: Color variants of the iris: a) blue, b) brown and c) green [5].

The next phase in the surface analysis procedure is to identify the interest regions. The iris surface is awe-inspiring and distinctive to everyone. When examined closely, the iris texture reveals radial furrows, which are areas of connective tissue that expand in a radial direction. According to the iridologist, a textural variation can emerge on the surface of the iris during life. Some textural variations might arise as early as the embryonic stage of iris formation. Rings, radial folds, and faults are the names given to these regions based on their shape and size [6]. Others have a lot of color diversity and are divided into darker and lighter areas or regions. Figure shows an example of several texture variants (3).

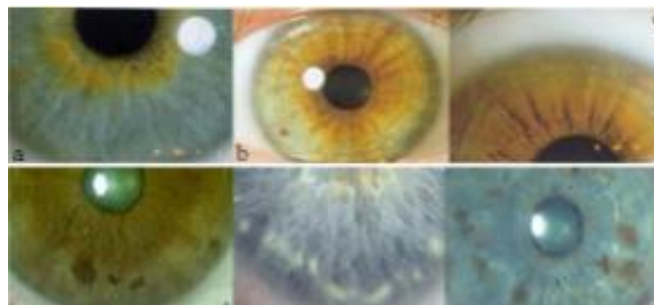


Figure 3: Spots On the iris, there are four types of spots: a) texture folds, b) texture rings, c) texture voltages, d) dark spots, and e) light spots: The same texture can be used for both dark and light pots [6].

The most recent advancements in the biometric research area, as well as the most recent image acquisition and processing techniques, may be able to provide incredibly beneficial solutions for iridology. It is possible to implement an automatic or semi-automatic biometric system for the encoding of eye images. In comparison to the visual iris evaluation tool, a computer-based analysis system has several advantages, including precision in identifying the boundaries of the iris, accurate color identification, exact chart matching, and accurate localization of specific iris regions (compared to the visual method). All these benefits contribute to increasing the accuracy of the final diagnosis [6]. The role of the user is critical in the system's operation. Based on this observation, the diagnosis system ought to be semi-automatic, in the sense that the final decision, the diagnosis, should be approved by the user before it is implemented.

In this study, the researchers hope to invent an automated biometric system, called the F.S. G-IRIDOLOGY, that will process eye images and prove that this system can diagnose 40 diseases in human body, as well as revealing the health status of skin and hair and many other functions. By creating an automated system for iris image acquisition and diagnosis. Algorithms and programs have also been developed to analyze the structure of the iris, as well as information about the color and pattern of the iris. The computer-based analysis system has several advantages, including accuracy in detecting the boundaries of the iris, determining the correct color, matching the histogram accurately, and localization of the areas of the

iris accurately. All of this takes less than a minute.

This paper also aims to demonstrate the efficacy of F.S.G. iridology in telemedicine settings through case studies. It is now easier than ever to screen a patient's health without needing to see a doctor, thanks to the development of mobile advanced technologies and data analysis tools. On the basis of this paper, we will investigate iris imaging as a diagnostic tool. Photos taken with a smart phone were analyzed in this way. As a result of this platform, we keep hoping to create a massive database of conventional iris images which are already labelled with medical information, as well as make it even easier to perform iris diagnosis research. the patient sends us a clear picture of their iris for both eyes (one picture for each eye) via social media. The device will then analyze the patient's iris images and provide information on the health status of the patient's body organs without needing an emplacement the patient to be in the clinic.

2. Materials and Methods

We have fabricated our device F.S.G. Iridology (FrequenSky Global) in our clinic frequensky global in malaysia by developing Dr. Daugmann's algorithm uses 3.4 bytes of data to represent iris information per square millimetre as explained in following section.

We have analysed the iris pictures by our F.S.G-Iridology for 385 patients, 142 of them were by telemedicine which come from several countries (Russia, Germany, U.S.A, Iraq, Syria, Lebanon, China, Japan, India, U.S.A., England, Germany, Italy and others) by sending their iris photos by social media. Other patients had come to our clinic frequensky global clinic in malaysia. The photo of patient`s iris has taken by our advice F.S.G IRIDOLOGY in distance of 3 inches from the eye.

This device is attached with a computer system as described below

2.1 First generation: Pure Visual Tools

As an iris detection instrument, a normal magnifying glass was initially used, and external ambient light was needed as the source for clearer vision. With the spread of applications, professional iris instruments have appeared, which still use pure optical magnifiers, but are equipped with detection lights, so that the iris can be clearly observed. Since regular magnifying lenses are very cheap and do not require a power supply, they can be used for any occasion, and there are still a few iris specialists who practice using them in some situations.

2.2 The second generation: Optical + electronic device

The optical instrument was developed together with electronic technology with the development of electronic technology, to become the second-generation iris instrument. It consists of optical components to form the lens of the iris instrument, the electronic components include signal acquisition/conversion

functions and even buffering, and are displayed by display equipment (professional color monitor, or color TV). It allowed to understand the iris, made this science (iris) more visible when explaining and testing, and greatly enhanced the education and popularization of the iris.

The second-generation iris instrument was developed later, with more functions, such as the freeze frame function: one or a few images can be cached for easy analysis and explanation; replacing lenses with different magnifications: the iris instrument equipped with photography and skin detection, and also a portable device with a small LCD screen.

The second-generation iris meter is widely used.

2.3 Third generation: optics + electronics + computer technology

The advent of computers greatly enhanced the development of society, and also introduced the iris meter in intelligence, so that more people could easily understand the application of iris diagnostics.

No professional training required in terms of diagnosis and automated computer analysis (iris processor), so no need for iris memorization. The USB interface is used to connect to the computer, no external power supply is required, and it can be used in different environments with a laptop.

2.4 The fourth generation: optics + electronics + computer technology + increasing pixels

The fourth-generation product has improved the pixels on the original basis. Currently, most of the pixels on the market are 300,000 pixels, and the resolution will be distorted after zooming in. The fourth-generation product increased its pixels to 1.3 million, which is a huge increase of one million pixels, the problem of image distortion.

3. Analysis and application

The professional lens is kind of 3D. Because the iris can accurately reflect the evaluation of the quality of body tissues, that is, the sub-health test, it is used in the auxiliary clinical test of beauty, health care and medical treatment, and it is widely used, and it is also a good health management method.

The lens of the device is a lens specially designed to capture improved iris images that cannot be distorted, can reproduce bright colors, clear and accurate images, and provide real image effects for iris analysis and judgment, and microvessels. It is the perfect combination for a comprehensive health check.

4. Data transfer

4.1 Computer input/output interface

The computer input/output interface is used for data,

information exchange and control between external equipment or user circuit and CPU. When we use it, the microcomputer bus must be used to connect the external device and the user circuit. At this time, the microcomputer bus interface must be used. The communication interface is used when a microcomputer system communicates directly with other systems. The bus interface is a kind of bus socket that provides the user with a microcomputer bus through the circuit socket to insert various functional cards. Each pin of the socket is connected to the corresponding signal line of the microcomputer bus. The user only needs to create the connection board of the external device or user circuit to the bus line sequence to achieve the connection of the external device or user circuit, and the system bus, or the user circuit and the microcomputer system become one.

Commonly used bus interface is AT bus interface, PCI bus interface, IDE bus interface, etc. The AT bus interface is mostly used to connect external devices in a 16-bit microcomputer system, such as a 16-bit sound card, a low-speed display adapter, a 16-bit data acquisition card, and a network card. The PCI bus interface is used to connect external devices in a 32-bit microcomputer system, such as 3D display cards, high-speed data acquisition cards, etc. The IDE bus interface is mainly used to connect various disks and optical drives, which can improve the data exchange speed and system capacity. Communication interface refers to the interface circuit for direct digital communication between the microcomputer system and other systems.

It is usually divided into two types: serial communication interface and parallel communication interface, that is, the serial port and the parallel port. The serial port is used to connect low-speed peripheral devices such as modems with small computers, the method of communication and information transmission one by one. The serial port standard is the RS-232C (Electronics Industry Association) standard. The serial port connector has nine Type D pins, a 25-pin socket, and D, which are located on the computer's main back panel out of the box. The mouse is connected to this serial port. Parallel interfaces are mostly used to connect high-speed peripheral devices such as printers, and the way to transfer information is in bytes, that is, 8 binary bits are executed at the same time.

4.2 Basic process

4.2.1 Input and Output BIOS and CMOS

BIOS is a collection of programs stored in EPROM on the motherboard's BIOS chip that primarily controls and manages the input/output system.

CMOS is a kind of system memory that stores the BIOS. It is a read-write ROM chip that is installed on the motherboard of a microcomputer. They are used to store the current configuration of the system's hardware and user preferences for certain parameters. When the computer is switched off, it

is powered by a battery to prevent the loss of data stored in memory. The user may utilize CMOS to configure the microcomputer's system settings. The BIOS is the motherboard's brain, since it is responsible for recognizing and controlling the functioning of different components and interfaces from the moment the computer starts up until the operating system is fully booted. Following booting of the operating system, the central processing unit (CPU) is responsible for the completion of different operations on storage devices and input/output devices, as well as power management for each component of the system.

4.2.2 Diagnosis through the iris

It is a professional medical product that diagnoses the health status of the body according to the color and density of fibers for different parts of the iris, and diagnoses 28 physiological phenomena of the human body. It guides us in early detection of disease, its causes and early treatment.

Developed by high-tech methods, the iris diagnosis device can accurately analyse the proportion of toxins and reveal the nature of the nutrition. The iris diagnosis device helps the nutritionist and cosmetologist to find out the cause and production of toxins and their deposition in the body, after the test, the patient can be given the appropriate medicine.

4.2.3 Iris analysis software (F.S.G-IRIDOLOGY)

It is a compact system based on the analysis of the iris by reading 12 transverse lines around the iris circle, which is a reversal of the nerves, the human body system, its organs and structure, detecting the status healthy of the skin and hair and many other functions.

From iris with a diameter of 11 mm, Dr. Daugmann's algorithm uses 3.4 bytes of data to represent iris information per square millimeter. In this way, the iris has about 266 quantitative feature points, while the general biometric technology has only 13 points. The iris recognition algorithm with 266 feature points is quantitatively described in several technical articles for iris recognition.

Dr. Daugmann indicated by his algorithm that 173 binary degrees of freedom can be obtained independently. In biometric technology, the number of this distinct point is very large.

4.2.4 Algorithm used

The first step is to locate the iris with a tiny camera about 3 inches from the eye. When the camera is aimed at the eye, the algorithm will gradually adjust the focus on the left and right sides of the iris to determine the outer edge of the iris. This horizontal method is obscured by the eyelids. The algorithm also focuses on the inner edge of the iris (the pupil) and removes the effect of eye fluid and fine tissue.

4.2.5 Iris Analyzer Data

- The Automatic Iris Atlas Diagnostic Device can use computer technology to capture images of the iris and automatically read it, the computer lists the relevant parts, shows the mechanism of the organs, and the energy ratio to know the symptoms and their causes, diseases, and their medication that are close to appearing. Customer data (name, age, gender, and address) can be managed.
- Automatic analysis and diagnosis of the client's iris.
- Comparative analysis: by analyzing the results by comparing images of the iris before and after treatment and during the treatment period.
- Store customer iris images and analysis results in the software.
- Print, preview, and archive the test report.
- Data, backup and restore functions, data is backed up and archived, backed up data can be restored by clicking restore data.
- Enlarge a part of the image with high resolution. To see more clearly, you can also change the position in which the enlarged image appears.
- Modify the content of the analysis and data while reading the case.
- View analysis, function.
- You can choose to display and hide the iris map.

4.2.6 Device Pros

- Easy to use for professionals
- No physical contact is required.
- High reliability.

4.2.7 Fields utilization of the device

- Institutes and Research.
- Health care centers.
- Health advice
- Nutritionist.
- Medicinal food workshop.
- Centers associated with the cosmetic and other health care industries.
- Health Product sales centers.

5. Diagnostic Results and Discussion

Automatic diagnosis device for iris atlas F.S.G. Iridology used a computer to capture images of the iris (left and right) and automatically read it, the computer lists the relevant parts, shows the mechanism of the organs, and the energy ratio to know the symptoms and their causes, diseases, and their medication that are close to appearing as shown as in figure 4 and table 1 which concern a male patient who is 63 years old.

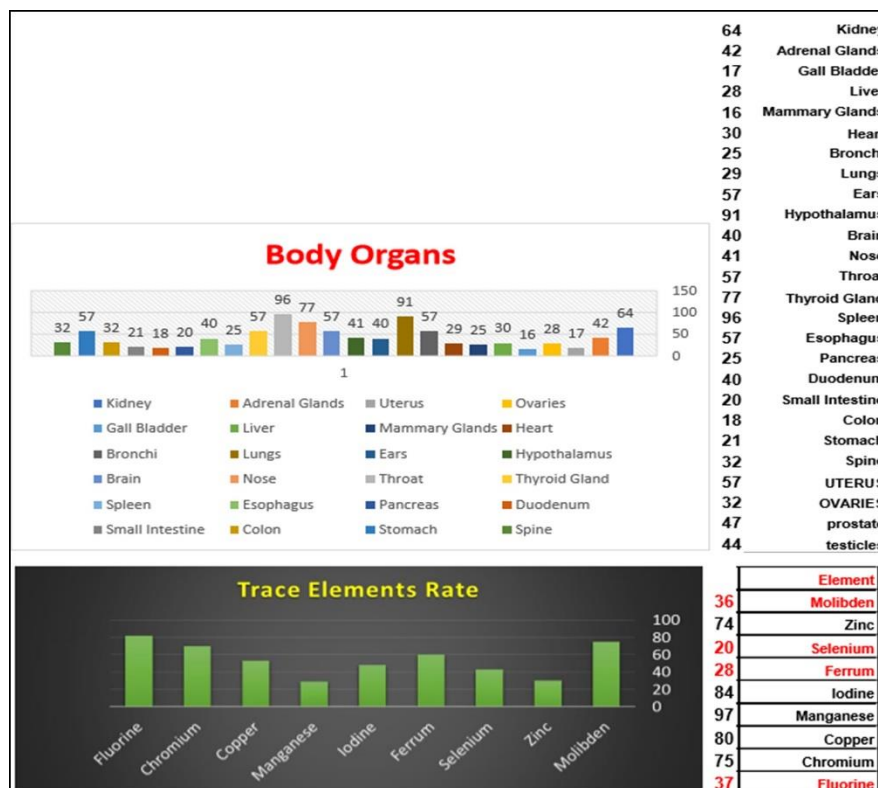


Figure 4: charts result of Diagnosis of body organs by F.S.G. Iridology and detecting all trace element rate in patient's body. Testing Time: 2020-01-15 18:59.

Table 1; Performance analysis of F.S.G. in appearing test results of patient's diagnosis by revealing the probably hidden problems and problem of sub-health trends. Reference Standard: Normal =; Moderately Abnormal ++; Moderately Abnormal --; Mildly Abnormal +; Mildly Abnormal -; Severely Abnormal +++; Severely Abnormal ---

System	Testing Item	Testing Result	Range
1-Kidney Function	Urobilinogen Index	Normal	=
	Uric acid Index	Moderately Abnormal	+
	Blood urea nitrogen (BUN) Index	Severely Abnormal	+
	Proteinuria Index	Moderately Abnormal	---
2-Liver function	Protein Metabolism	Normal	=
	Energy Production Function	Abnormal	-
	Detoxification Function	Moderately	+
	Bile Secretion Function	Normal	=
	Liver Fat Content	Mildly Abnormal	-
3-Rheumatoid bone disease	Osteoporosis Coefficient	Moderately Abnormal	++
4-Prostate	Prostatitis	Moderately Abnormal	---
	Syndrome	Normal	+
	Degree of Prostatic Hyperplasia	Mildly Abnormal	---
	Degree of Prostatic Calcification	Moderately Abnormal	++
5-Allergy	Animal fur allergy index	Moderately Abnormal	+
6-Cardiovascular and cerebrovascular	Vascular Elasticity	Severely Abnormal	+++
7-Gastrointestinal function	Pepsin Secretion Coefficient	Moderately Abnormal	+
	Gastric Peristalsis Function Coefficient	Moderately Abnormal	---
	Gastric Absorption Function Coefficient	Moderately Abnormal	++
	Small Intestine Peristalsis Function Coefficient	Normal	=
	Small Intestine Absorption Function Coefficient	Severely Abnormal	+
8-Gallbladder function	Alkaline Phosphatase (ALP)	Normal	=
	Bilirubin (DBIL)	Moderately Abnormal	+
	Serum Globulin (A/G)	Normal	=
	Total Bilirubin (TBIL)	Severely Abnormal	-
	Serum Total Bile Acid (TBA)	Moderately Abnormal	+
9-Pancreatic function	Insulin	Moderately Abnormal	---
	Pancreatic Polypeptide (PP)	Normal	=
	Glucagon	Mildly Abnormal	+
10-Lung function	Total Lung Capacity TLC	Normal	=
	Arterial Oxygen Content PaCO2	Normal	=
	Airway Resistance RAM	Severely Abnormal	+
	Vital Capacity VC	Moderately Abnormal	---
11-Brain nerve	Memory Index (ZS)	Mildly Abnormal	+
12-Bone mineral density	Amount of Calcium Loss	Mildly Abnormal	---
	Non-Mineral Density	Moderately Abnormal	---
13-Endocrine System	Adrenal glands Index	Normal	=
14-Immune System	Lymph node Index	Mildly Abnormal	---
15-Eye	Collagen eye wrinkle	Mildly Abnormal	---
	Sagging	Mildly Abnormal	---
16-Coenzyme	Nicotinamide	Severely Abnormal	---
	Folic acid	Mildly Abnormal	---
	Biotin	Mildly Abnormal	---
	Pantothenic acid	Normal	=
	Glutathione	Mildly Abnormal	---
	Hyperinsulinemia coefficient	Normal	+
17-Thyroid	Triglyceride content of abnormal coefficient	Mildly Abnormal	---
	Free thyroxine (FT4)	Normal	=
	Anti-thyroglobulin antibodies	Normal	=
	Three triiodothyronine (T3)	Normal	=
	Free thyroxine (FT4)	Normal	=
	Hand-Shao yang triple burner	Mildly Abnormal	---
	Foot Gallbladder	Normal	---

18-Channels and collaterals	Foot Jue Yin Liver	Mildly Abnormal	+
19-Pulse of heart and brain	Pulse wave coefficient K	Mildly Abnormal	—
20-Blood lipids	Total, cholesterol (TC)	Severely Abnormal	+
	Low-density lipoprotein (LDL-C)	Mildly Abnormal	+
	Circulating immune complex (CIC)	Normal	=
21-Vitamins	Vitamin B1	Mildly Abnormal	+
	Vitamin C	Mildly Abnormal	++
	Vitamin E	Mildly Abnormal	—
	Vitamin K	Normal	=
22 - Trace element	Iodine	Severely Abnormal	+
	Strontium	Normal	+
	Calcium	Severely Abnormal	+
	Selenium	Normal	=
	Potassium	Mildly Abnormal	+
	Iron	Normal	=
24-Heavy Metal	Lead	Mildly Abnormal	+
	Arsenic	Normal	=
	Thallium	Moderately Abnormal	+
25-Human toxin	Toxic Pesticide	Mildly Abnormal	+
	Stimulating Beverage	Severely Abnormal	—
	Electromagnetic Radiation	Normal	=
	Tobacco / Nicotine	Severely Abnormal	—

5.1 Function of the kidneys

The F.S.G. shows a severely abnormal Blood urea nitrogen (BUN) Index. When urea nitrogen levels are elevated, it indicates that the kidneys are not functioning properly due to dehydration, shock, or a high-protein diet. He also needs to pay attention to the side effects of the drugs he's taking (table 1).

We have diagnosed 385 patients, of whom 101 (26.24%) (table 2) had a severely abnormal Urobilinogen Index, compared to 96 (24.95%) who had a high uric acid index and 93 (24.16%) who had a severely abnormal proteinuria index. The average proteinuria index is normal in 43.90 % of our patients, and the blood urea nitrogen index is normal in 36.89 %, while the uric acid and urobilinogen indexes are abnormal in 29.36 % and 26.49 %, respectively (table 2). There was a spot of light on the party that related to kidney with a precision of 98.20% due to uncleared images shared on social media (7 photos/385).

This is similar to the findings of Sare Amerifar et al., who studied human iris samples. This research made use of the CASIA eye image database. CHT has been used to obtain circular forms, while Hessian assessment is used to enhance geometric shapes' accurateness [7].

The Intelligent Iris-based Chronic Kidney Identification System was used by Muzamil et al. as an alternative medical diagnostic method (ICKIS). Using an artificial intelligence algorithm and iridology, ICKIS was able to detect chronic kidney disease in its early stages. A deep neural network-based algorithm analyzes the subject's iris to see if they have a chronic kidney problem. If they do, the ICKIS can tell them. According to ICKIS research, the device correctly classified over 2000 people as having either healthy kidneys or chronic kidney disease with an accuracy rate of 96.8 percent [8].

In a study conducted by Hussain et al. [9], the effectiveness of

iridology in detecting renal diseases was evaluated using artificial intelligence. Researchers looked at data from 168 people in good health and 172 people with chronic renal failure. They correctly identified 82% of the normal patients and 93% of the renal patients. The method's effectiveness was tested on a patient with a systemic disease that manifested as ocular symptoms.

All research into developing a new system for the identification of kidney diseases gives a general state of kidney health, and no research until now has been able to determine all kidney function indices (Urobilinogen, Uric acid, Blood urea nitrogen, and Proteinuria Index) as F.S.G iridology.

5.2 Cardiovascular and cerebrovascular

Unfortunately, the Vascular Elasticity was severely abnormal, which supposes that our patient will have a healthy heart problem (table 1, figure 4). When we compared the vascular elasticity of 385 patients diagnosed by our F.S.G device with that of healthy hearts, we found that 101 of them had abnormal elasticity, while 174 had healthy hearts (table 2), meaning that the designed system can detect early heart function problems using the Iridology method, with success rates of 100 percent by using the F.S.G iridology. This finding is in line with that of Leonardus et al. [10], who used the test results of PCA (Principal Component Analysis) score variation to see if the PCA score affected the rate at which early heart problem symptoms were recognized. The designed system could work well with image processing, feature extraction with PCA, and classification with a Backpropagation Neural Network. As many as few PCA score variations were tested such as 600, 500, 400, 300 and 200 on 40 test data, yielding a success rate of 92.5 %, 90 %, 85 %, 75% and 67.5 % respectively. Although

Benedictor A. et al. [11] is in accord with our results. He proposed an IFB-method (Iris Features-Based Heart Disease). The processing results of IFB-method infer that the characteristic of iris tissue leads to accurate detection of early stage and premature abnormalities in heart.

5.3 Liver Function

There is a severe deficiency in energy due to a dysfunction of the liver. Table 1 shows the results of F.S.G. Iridology's analysis of liver functions, including protein metabolism, energy production, detoxification, bile secretion, and fat content. Except for the abnormally high fat content, all these measurements were within the normal range (Table 1). The study's limitations are also evident in the small sample of iris specimens that could be analysed after five photographs were discarded because of poor image quality.

The validity of this approach was examined in 385 liver patients, with a detection accuracy of 98.70 percent. Protein metabolism was normal in 204 people, while it was severely abnormal in the other 51, and the energy production section was normal in 213 patients, detoxification was healthy in 205 people, and bile secretion was normal in 198 others. In contrast, the energy production function was severely abnormal in 65 people, detoxification was unhealthy in 57, and bile secretion was abnormal in 89 people (table 2).

Hareva et al. [12] created an iridology app that analyses an individual's iris image to determine their health status. However, it was integrated into an Android-based smartphone. The heart, spine, kidneys, and lungs were identified as the four organs in question. It was evident from the results whether the member was in good health. Without revealing any more details about the individual organs.

In the iris image, Herlambang et al. [13] introduced liver disease. It was proposed that a back-propagation neural network and a grey level co-occurrence matrix (GLCM) be used for feature extraction to detect liver disease. They built a liver disorder diagnosis app in Matlab. The researchers examined the right eye iris images of 60 people, 34 of whom had normal iris images and 26 of whom had abnormal ones.

5.4 Gastro-intestinal function

Gastric peristalsis, absorption, and secretion function coefficients were moderately abnormal in (table 1), but the small intestine absorption function coefficient was severely abnormal, even though small intestine peristalsis was in good health. A healthy pepsin secretion coefficient is found in 55.32 percent (n: 213/385) of patients, while a severely abnormal one is found in 26.24 % (table 2), so, 52.73 % (n: 203/385) of patients have a normal Gastric Peristalsis Function Coefficient, while 25.45 % (n: 213/385) of patients have a dysfunctional one (table 2). 12.21% of patients have a severely abnormal Small Intestine Peristalsis Function Coefficient, while 14.55% of patients have an abnormal Small Intestine Absorption

Function Coefficient, while this percent is increased to 49.09% and 53.51 % for a healthy and normal Small Intestine Peristalsis Function Coefficient and Small Intestine Absorption Function Coefficient, respectively (table 2).

Using iris images and image processing concepts, our findings is in line with Miranda et al [14]. When it comes to diagnosing digestive tract diseases like diverticulitis and diverticulitis with transverse colon prolapse, they developed an algorithm technique using human iris parameters. A larger study is needed to determine the success or failure of this experiment. Carrera et al. [15] proposed a browser specific diagnostic system that is based on iridology for the early identification of digestive problems. System components include machine learning algorithms and image processing methods. The system was tested on 100 images acquired and demonstrates a highest accuracy of 96 % and a predictive capacity of 99 %. According to the findings of this research, complementary and alternative medicine techniques have diagnostic potential for gastrointestinal health issues as well.

5.5 Lungs

Table 1 shows that our patient's TLC (Total Lung Capacity) and PaCO₂ (Arterial Oxygen Content) are both normal, but his vital capacity (VC) is slightly below normal. In spite of this, he was severely subnormal due to severe damage to his Airway Resistance RAM. One-quarter had significant damage to their TLC, while the other two-thirds had an otherwise healthy TLC. However, 24.16 % have an abnormal VC and 49.35 % have a normal one (table 2). All images were enhanced, and the results were flawless. This finding is consistent with that of Anna et al. [16] They developed Adaptive Resonance Theory 1 (ART1), a sort of artificial neural system that contains unregulated deep learning to evaluate lung illnesses via iris images. A lung imbalance detection system based on iris segmentation and color dissimilarity extraction was developed in this paper. It uses ART1's input to transform the iris image into the lung and pleura representation region, and then the ART1 neural network framework recognizes patterns in the iris image. ART1 is regarded as one of the most resilient and adaptable solutions in the ever-changing world of pattern recognition. We concur with Hussain et al. [17], who proposed an iris algorithm for noninvasively diagnosing obstructive lung disease (OLD). In order to detect lung disorders, they created a real-time iris-based pre-diagnostic system that uses a machine learning algorithm and an iridology chart. A Gabor filter and a support vector machine were used to extract the features (SVM). The accuracy of the system in detecting lung disorders was 88% in this study, which included 50 lung patients and 50 healthy subjects.

5.6 Rheumatoid bone disease

Patients with rheumatoid arthritis who had osteoporosis had a slight increase in their energy levels when compared to

standard, according to F.S.G. iridology (table 1). F.S.G. diagnosed 385 patients, and found that 69.35% had a healthy osteoporosis coefficient, while 12.74% had disease in their osteoporosis coefficient. Two images were discarded because of the presence of a light spot in the region responsible for the detection of rheumatoid bone disease. However, the accuracy of F.S.G. Iridology IS 99.48%. (table 2). There hasn't been any research to date showing how iridology can help diagnose rheumatoid bone disease.

5.7 Prostate

F.S.G Iridology shows that the prostatitis was moderately reduced from the standard, while the syndrome was normal and the degree of Prostatic Hyperplasia was close to a healthy level, despite the fact that the degree of Prostatic Calcification was moderately elevated (table 1). We found that 63.08 % (123 out of 195 men) had a good healthy level of prostatitis, compared to 48.72 percent of patients who had a good level of significance in Degree of Prostatic Hyperplasia, while the significance level in detecting the abnormality of the Prostatitis organ was 18.97 % out of 195 patients, compared to 25.13 % of patients who had a severely abnormal Degree of Prostatic Hyperplasia. Prostate disorders were discovered thanks to the experiment, which demonstrated a precision of 100 percent (table 2). In detecting prostate diseases through iridology, no other study has come close to matching our success rate.

5.8 Allergy

Our patient has a moderate animal skin allergy index (Table 1). There is no research on using iridology to diagnose allergy disease. Table 2 shows that 31.43 % of the 385 patients have

no allergy symptoms while 29.35 % have a severe allergy to animal fur allergy index, as shown. This result demonstrates a diagnostic accuracy rate of one hundred percent for all allergy indexes (table 2).

5.9 Thyroid

Anti-thyroglobulin antibodies, free thyroxine (FT4), and three triiodothyronine (T3) levels, as well as thyroglobulin levels, all fell within the normal range for patient (table 1). Iris' thyroid gland had gone undiagnosed until now due to a lack of previous research. Patients with healthy Anti-thyroglobulin antibodies (212 out of 385) have a higher percentage of good triiodothyronine (44.42 %) than those with abnormally low levels of T3, as shown in table 2.

5.10 Pancreatic function

Insulin levels were slightly higher than normal, and Pancreatic Polypeptide (PP) appeared to be working properly (table 1). Glucagon levels are normal in 49.61 % (191 patients from 385), while Pancreatic Polypeptide (PP) levels are normal in 45.97 % (177/285), while the disease prevalence is abnormal in 24.15 % (93/385) and 24.68 % (95/385), respectively. According to Wibawa et al. [18], who used statistical analysis on 34 iris data points, this result is in agreement with theirs. It's highly significant to detect 94% of patients with broken tissue and 100% of those with Pancreas organ anomaly from 34 patients, as well as the presence of broken tissue. Iris diagnosis was used by Lesmana et al. [19] to gauge insulin levels in the blood. Their study's results show an accuracy rate of 83.3%, and they assisted in the discovery of pancreatic disorders.

Table 2: Performance analysis of F.S.G. in appearing test results of 385 patient's diagnosis (195 men and 190 women). The testing accuracy (%) of diagnosis results. Reference Standard: Normal =; Moderately Abnormal ++; Moderately Abnormal --; Mildly Abnormal +; Mildly Abnormal -; Severely Abnormal ++++; Severely Abnormal ---.

System	Testing Item	Number of patients for Testing Result				N° of Unclear Images	Testing Accuracy (%)
		Normal =	Severely Abnormal ---- or ++++	Moderately Abnormal -- or ++	Mildly Abnormal -or +		
1-Kidney Function	Urobilinogen Index	113	101	81	83	7	98.20 %
	Percent (%)	29.36 %	26.24 %	21.03 %	21.55 %		
	Uric acid Index	102	96	113	67		
	Percent (%)	26.49 %	24.95 %	29.36 %	17.40 %		
	Blood urea nitrogen (BUN) Index	142	73	94	69		
	Percent (%)	36.89 %	18.96 %	24.43 %	17.92 %		
	Proteinuria Index	169	93	45	71		
Percent (%)	43.90 %	24.16 %	11.70 %	18.44 %			
2-Liver function	Protein Metabolism	204	51	59	66		
	Percent (%)	52.99 %	13.25 %	15.32 %	17.14 %		
	Energy Production Function	213	65	53	49		
	Percent (%)	55.32 %	16.88 %	13.77 %	12.73 %		
	Detoxification Function	205	57	37	81		
	Percent (%)	53.24 %	14.81 %	9.61 %	21.04 %		
Bile Secretion Function	198	89	29	64			

	Percent (%)	51.43 %	23.12 %	7.53 %	16.62 %	5	98.70 %
	Liver Fat Content	209	75	51	45		
	Percent (%)	54.29 %	19.48 %	13.25 %	11.68 %		
3-Rheumatoid bone disease	Osteoporosis Coefficient	267	48	36	32	2	99.48 %
	Percent (%)	69.35 %	12.47 %	9.35 %	8.31 %		
4-Prostate	Prostatitis	123	37	16	19	0	100 %
	Percent (%)	63.08 %	18.97 %	8.21 %	9.74 %		
	Syndrome	98	59	23	15		
	Percent (%)	50.26 %	30.26 %	11.79 %	7.69 %		
	Degree of Prostatic Hyperplasia	95	49	17	34		
	Percent (%)	48.72 %	25.13 %	8.71 %	17.44 %		
	Degree of Prostatic Calcification	89	39	31	36		
Percent (%)	45.64 %	20.00 %	15.90 %	18.46 %			
5-Allergy	Animal fur allergy index	121	113	102	49	0	100 %
	Percent (%)	31.43 %	29.35 %	26.49 %	12.73 %		
6-Cardiovascular and cerebrovascular	Vascular Elasticity	174	101	32	78	0	100 %
	Percent (%)	45.20 %	26.23 %	8.31 %	20.26 %		
7-Gastrointestinal function	Pepsin Secretion Coefficient	213	101	48	23	0	100 %
	Percent (%)	55.32 %	26.24 %	12.47 %	5.97 %		
	Gastric Peristalsis Function Coefficient	203	98	27	57		
	Percent (%)	52.73 %	25.45 %	7.01 %	14.81 %		
	Gastric Absorption Function Coefficient	199	115	56	15		
	Percent (%)	51.69 %	29.87 %	14.55 %	3.89 %		
	Small Intestine Peristalsis Function Coefficient	189	47	91	58		
	Percent (%)	49.09 %	12.21 %	23.64 %	15.06 %		
	Small Intestine Absorption Function Coefficient	206	56	55	68		
Percent (%)	53.51 %	14.55 %	14.29 %	17.65 %			
8-Gallbladder function	Alkaline Phosphatase (ALP)	235	36	27	87	0	100 %
	Percent (%)	61.04 %	9.35 %	7.01 %	22.60 %		
	Bilirubin (DBIL)	224	39	32	90		
	Percent (%)	58.19 %	10.13 %	8.31 %	23.37 %		
	Serum Globulin (A/G)	241	41	42	61		
	Percent (%)	62.60 %	10.65 %	10.91	15.84		
	Total Bilirubin (TBIL)	274	33	28	50		
	Percent (%)	71.17 %	8.57 %	7.27 %	12.99 %		
	Serum Total Bile Acid (TBA)	288	41	40	16		
Percent (%)	74.81 %	10.64 %	10.39 %	4.16 %			
9-Pancreatic function	Insulin	192	95	59	39	0	100 %
	Percent (%)	49.87 %	24.68 %	15.32 %	10.13 %		
	Pancreatic Polypeptide (PP)	177	95	65	48		
	Percent (%)	45.97 %	24.68 %	16.88 %	12.47 %		
	Glucagon	191	93	52	49		
Percent (%)	49.61 %	24.15 %	13.51 %	12.73 %			
10-Lung function	Total Lung Capacity TLC	163	88	79	55	0	100 %
	Percent (%)	42.34 %	22.86 %	20.52 %	14.28 %		
	Arterial Oxygen Content PaCO2	144	97	83	61		
	Percent (%)	37.40 %	25.19 %	21.56 %	15.85 %		
	Airway Resistance RAM	177	79	78	51		
	Percent (%)	45.97 %	20.52 %	20.26 %	13.25 %		
	Vital Capacity VC	190	93	60	42		

	Percent (%)	49.35 %	24.16 %	15.58 %	10.91 %		
11-Brain nerve	Memory Index (ZS)	233	21	59	72	0	100 %
	Percent (%)	60.52 %	5.45 %	15.33 %	18.70 %		
12-Bone mineral density	Amount of Calcium Loss	209	40	43	93	0	100 %
	Percent (%)	54.28 %	10.39 %	11.17 %	24.16 %		
	Non-Mineral Density	249	55	33	48		
	Percent (%)	64.68 %	14.28 %	8.57 %	12.47 %		
13-Endocrine System	Adrenal glands Index	216	37	81	51	0	100 %
	Percent (%)	56.10 %	9.61 %	21.04 %	13.25 %		
14-Immune System	Lymph node Index	227	13	76	69	0	100 %
	Percent (%)	58.96 %	3.38 %	19.74 %	17.92 %		
15-Eye	Collagen eye wrinkle	189	100	66	30	0	100 %
	Percent (%)	49.09 %	25.97 %	17.14 %	7.80 %		
	Sagging	199	87	59	40		
	Percent (%)	51.69 %	22.60 %	15.32 %	10.39 %		
16-Coenzyme	Nicotinamide	168	98	58	61	0	100 %
	Percent (%)	43.64 %	25.45 %	15.06 %	15.85 %		
	Folic acid	264	52	34	35		
	Percent (%)	68.57 %	13.51 %	8.83 %	9.09 %		
	Biotin	134	57	74	120		
	Percent (%)	34.81 %	14.81 %	19.22 %	31.17 %		
	Pantothenic acid	198	49	67	71		
	Percent (%)	51.43 %	12.73 %	17.40 %	18.44 %		
	Glutathione	204	57	55	69		
	Percent (%)	52.99 %	14.81 %	14.29 %	17.91 %		
	Hyperinsulinemia coefficient	199	23	84	79		
	Percent (%)	51.69 %	5.97 %	21.82 %	20.52 %		
	Triglyceride content of abnormal coefficient	159	119	67	40		
	Percent (%)	41.30 %	30.91 %	17.40 %	10.39 %		
17-Thyroid	Anti-thyroglobulin antibodies	212	71	33	69	0	100 %
	Percent (%)	55.07 %	18.44 %	8.57 %	17.92 %		
	Three triiodothyronine (T3)	171	49	84	81		
	Percent (%)	44.42 %	12.73 %	21.82 %	21.03 %		
	Free thyroxine (FT4)	194	39	60	92		
	Percent (%)	50.39 %	10.13 %	15.58 %	23.90 %		
	Thyroglobulin	177	52	57	99		
Percent (%)	45.97 %	13.51 %	14.81 %	25.71 %			
18-Channels and collaterals	Hand-Shao yang triple burner	201	47	52	85	0	100 %
	Percent (%)	52.21 %	12.21 %	13.50 %	22.08		
	Foot Gallbladder	223	25	33	104		
	Percent (%)	57.92 %	6.49 %	8.57 %	27.02 %		
	Foot Jue Yin Liver	216	31	29	109		
Percent (%)	56.11 %	8.05 %	7.53 %	28.31 %			
19-Pulse of heart and brain	Pulse wave coefficient K	191	88	55	51	0	100 %
	Percent (%)	49.61 %	22.86 %	14.28 %	13.25 %		
20-Blood lipids	Total, cholesterol	159	119	67	40	0	100 %
	Percent (%)	41.30 %	30.91 %	17.40 %	10.39 %		
	Low-density lipoprotein (LDL-C)	188	86	45	66		
	Percent (%)	48.83 %	22.34 %	11.69 %	17.14 %		
	Circulating immune complex (CIC)	199	70	42	74		
Percent (%)	51.69 %	18.18 %	10.91 %	19.22 %			
21-Vitamins	Vitamin B1	336	11	15	23	0	100 %
	Percent (%)	87.27 %	2.86 %	3.90 %	5.97 %		
	Vitamin C	215	66	51	53		
	Percent (%)	55.84 %	17.14 %	13.25 %	13.77 %		
	Vitamin E	289	41	47	8		
Percent (%)	75.07 %	10.65 %	12.21 %	2.07 %			

	Vitamin K	303	14	9	59		
	Percent (%)	78.70 %	3.64 %	2.34 %	15.32 %		
22-Trace element	Iodine	298	32	17	38	0	100 %
	Percent (%)	77.40 %	8.31 %	4.42 %	9.87 %		
	Strontium	309	42	11	23		
	Percent (%)	80.26 %	10.91 %	2.86 %	5.97 %		
	Calcium	199	89	69	28		
	Percent (%)	51.69 %	23.12 %	17.92 %	7.27 %		
	Selenium	203	21	50	111		
	Percent (%)	52.73 %	5.45 %	12.99 %	28.83 %		
	Potassium	219	54	42	70		
	Percent (%)	56.88 %	14.03 %	10.91 %	18.18 %		
23- Heavy Metal	Iron	189	91	66	39	0	100 %
	Percent (%)	49.09 %	23.64 %	17.14 %	10.13 %		
	Lead	324	17	13	31		
	Percent (%)	84.16 %	4.41 %	3.38 %	8.05 %		
	Arsenic	335	13	15	22		
	Percent (%)	87.01 %	3.38 %	3.90 %	5.71 %		
24- Human toxin	Thallium	349	11	9	16	0	100 %
	Percent (%)	90.65 %	2.86 %	2.34 %	4.15 %		
	Toxic Pesticide	351	19	05	10		
	Percent (%)	91.17 %	4.93 %	1.30 %	2.60 %		
	Stimulating Beverage	124	115	87	59		
	Percent (%)	32.21 %	29.87 %	22.60 %	15.32 %		
	Electromagnetic Radiation	164	78	42	101	0	100 %
	Percent (%)	42.60 %	20.26 %	10.91 %	26.23 %		
	Tobacco / Nicotine	133	101	64	87		
	Percent (%)	34.55 %	26.23 %	16.62 %	22.60 %		

5.11 Brain nerve

The memory index (ZS) is within the normal range, according to the F.S.G. brain scan results (table 1).

Sixty-five percent of patients (233/385) have a normal memory index, while fifteen percent (53/385) have a moderate memory index. The accuracy rate is one hundred per cent (table 2). These findings cannot be compared to anything else.

5.12 Bone mineral density

In terms of bone mineral density, we were able to demonstrate that there was a small amount of calcium loss and non-mineral density that was slightly abnormal (table 1). A normal calcium loss rate is found in 54.28 percent of patients, while a severely abnormal rate is found in just 10.39 percent. The accuracy rate is one hundred per cent. This is the first device in iridology to detect changes in bone mineral density based on changes in the color of the eyeballs.

5.13 Eye

All index of eyes (Collagen eye wrinkle, Sagging) (table 1) were mildly subnormal, because they were a little lower than normal. While 49.09 %, 51.69 % of patients are in the healthy range compared to 25.97 % and 22.60 % which have an abnormal level.

We are the first researchers who have successively diagnosed the Collagen eye wrinkle and sagging by iris images with accuracy of 100 %.

5.14 Coenzyme

F.S.G shows that the healthy level of Biotin, Glutathione, Triglyceride coefficient were mildly abnormal. While the Pantothenic acid, Folic acid, Hyperinsulinemia coefficients are in healthy state. Therefore, the nicotinamide is highly elevated due to smoking (table 1).

As seen in table 2: 25.45 %, 13.51 %, 14,81 %, 12.73 %, 14.81 %, 5.97 % and 30.91% of patients have a severely abnormal level of Nicotinamide, Folic acid, Biotin, Pantothenic acid, Glutathione, Hyperinsulinemia coefficient and Triglyceride content of abnormal coefficient respectively. With an accuracy of 100 %.

We didn't find a study about diagnosis the coenzyme by iridology to be compared with our results.

5.15 Channels and collaterals

Hand-Shao yang triple burner and Foot Jue Yin Liver were mildly abnormal (table 1), nevertheless the Foot Gallbladder was healthy. 52.21 % patients have healthy level and 12.21 % unhealthy level of Hand-Shao yang triple burner (table 2). The accuracy of channels and collaterals is 100 % (table 2). No

precedent study was made for detecting Channels and collaterals by iridology.

5.16 Pulse of heart and brain

The Pulse wave coefficient K was less than normal (table 1). In our research we find 49.61 % of patients have a normal Pulse of heart and brain compared to 22.86 % have a severely abnormal level. There is no study to be compared with our results.

5.17 Blood lipids

F.S.G reveals to us that the patient has a high percentage of cholesterol (TC) (table1), while the Low-density lipoprotein (LDL-C) was slightly higher than normal. However, only that Circulating Immune Complex (CIC) was normal.

Table 2 shows that 30.91 % of patients have elevated total cholesterol, whereas 22.34 % have aberrant low-density lipoprotein (LDL-C) and 18.18 % have elevated levels of circulating immune complex. F.S.G. is 100 % accurate when it comes to identifying blood lipids.

As previously reported by BurakK ürşatGül et al. [20], iris pictures are quite beneficial in the medical area. These photos were utilized to determine the patient's health and, as a result, the body's tissue structure. The authors of this study investigated the link between high levels of cholesterol in human blood and the formation of a sodium ring around the iris. There were several stages to the process described above. Pupils in the first grade have been identified the iris in a black-and-white. In the second stage, determine the diameter of the sodium ring around the iris based on the image's color quality analysis. The results of the experiment showed a correlation between the concentration of cholesterol in a human blood sample and the diameter of the sodium ring.

5.18 Endocrine System

The patient had a normal Adrenal Glands Index (table 1). No study was found to be compared of our results.

5.18.1 Immune System

Lymph node Index was lower than the normal range (table 1). During diagnosis 385 patients, there were 227 patients having a good Lymph Node Index, while 13 only 13 patients have a very low Lymph Node Index (table 2) with an accuracy of 100 %.

5.18.2 Gallbladder function

F.S.G iridology demonstrates that our patient has a health problem in his gallbladder because the average total bilirubin (TBIL) was much lower than the standard range. Nevertheless, A/G and Alkaline Phosphatase (ALP) were in a healthy range.

Finally, the Serum Total Bile Acid (TBA) and Bilirubin (DBIL) were both somewhat abnormal as shown in Table 1. Between 385 patients, the F.S.G. detects 36 patients with a high level of Alkaline Phosphatase (ALP) (table 2), 39 patients with an abnormal level of Bilirubin (DBIL), and 33 patients with a bad problem in Total Bilirubin (TBIL) (table 2). Knipschild [21] came to the opposite conclusion, saying iridology is a useless diagnostic tool. He took stereo color slides of the right eye and developed them. A total of 39 patients with gallbladder disease and 39 healthy controls had stereo color slides prepared of the right eye. Five eminent iridologists were shown the slides in a random order with no more explanation.

5.19 Vitamins

F.S.G. successively detected the content of multiple vitamins in the human body. Table1 reveal that our patient has mildly abnormal quantities of vitamins C, B1, E. so the percent of vitamin k in his body is in an acceptable range. Iris images of 385 patients see that 87.27 %, 55.84%, 75.07% and 78.70% have a normal level in quantity of vitamins B1, C, E, K, respectively. Therefore, unfortunately, 2.86 %, 17.14 %, 10.65 %, 3.64% suffers from a deficiency of vitamins B1, C, E, K, respectively. Accuracy detecting vitamins in human body by F.S.G. is 100 % (table 2).

5.20 Trace elements

Some minerals in human body have been very successfully identified by F.S.G. Iridology. Table 1 shows the hard deficiency of calcium for our patient, however potassium is mildly abnormal, while the selenium and iron are in standard average.

As shown as in table 2, F.S.G. has identified quantities of some minerals in patients 'body like Iodine, Strontium, Calcium, Selenium, Potassium and Iron; the accuracy for detecting trace elements is 100 %.

5.21 Heavy metals

In addition to discovering all the above, F.S.G. has detected heavy metals in human body as shown in tables1 and 2. The patient in table 1 has a moderately abnormal in quantity of lead and thallium in his body, while the percent of arsenic is in standard level (table 1). There were 4.41%, 3.38 and 2.86% between 385 patients had an abnormal level of lead, arsenic, and thallium respectively (table 2).

5.22 Human toxin

Unfortunately, there were 4.93%, 29.87%; 20.26% and 26.23 % of patients have an excessively level of Toxic Pesticide, Stimulating Beverage, Electromagnetic Radiation, Tobacco / Nicotine respectively with an accuracy 100 %.

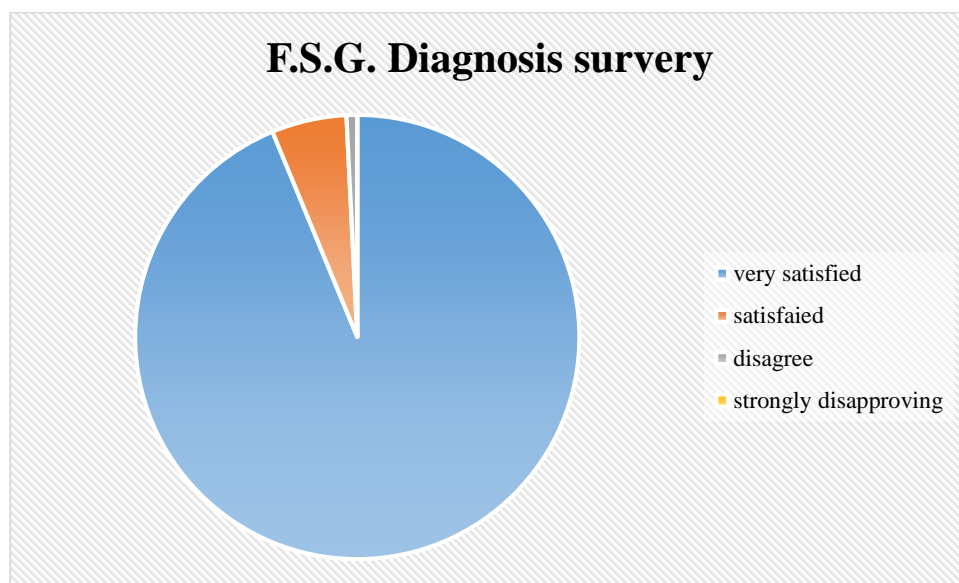


Figure 5: Referendum diagnosis on endorsement, efficacy and trustworthiness of F.S.G. iridology application

364 patients strongly agreed to use F.S.G. Iridology as shown in Figure 5, because they felt, all their diagnoses are accurate based on their current disease. They found it very helpful to heal the patient due to short time required to reveal all diseases of patients (59 secs only).

6. Conclusions

F.S.G. Iridology is considered as revolution in iridology science as it is the first time we have been able to develop an iridology device for diagnosing and detecting the health status of several body's organs as: Kidney, Adrenal Glands, Gall Bladder, Liver, Mammary Glands, Heart, Bronchi, Lungs, Ears, Hypothalamus, Brain, Nose, Throat, Thyroid Gland, Spleen, Oesophagus, Pancreas, Duodenum, Small intestine, Colon, Stomach, Spine, Uterus, Ovaries, Prostate, Testicles, in addition to determination trace elements rate (fluorine, chromium, copper, manganese, iodine, iron and selenium) and some vitamins like B1, C, E, K. all these diagnosing is only in one minute with accurate of 100%. That avoids some diseases which require highest speed in diagnosis to prevent a dangerous outcome, accurate, cheap, and fast diagnosis can save many lives from inevitable danger. In addition, the diagnosis by F.S.G is cost-effective, robust, reliable, non-contact, non-radioactive and convenient by involving computer vision on iridology to characterize abnormalities in iris features.

References

[1] N.A. Menzies, C. Ted, L. Hsien-Ho, M. Murray and J. A. Salomon, "Population health impact and cost-effectiveness of tuberculosis diagnosis with xpert mtb/rif: a dynamic simulation and economic evaluation, *plos medicine*, Volume. 9 Issue 11 Nov. 2012, e1001347 1-17.

[2] S. Allie, D. M Worthen, and J. A. Mitas, "An evaluation of iridology, *Jama*, Volume. 9 Issue 13 Sep. 1979, 1385-1389.

[3] D. Gayle, "The eyes have it: The iris pictured in remarkable detail by incredible close-up shots, <http://www.dailymail.co.uk/sciencetech/article-2246888/The-eyes-The-iris-pictured-remarkable-incredible-close-shots.html>, Dec. 2012.

[4] R. M Holl, "Iridology: another look, *journal of Alternative health practitioner*, vol. 5 issue 1, spring 1999,35-43.

[5] S. Demea, "Correlations between iris aspects and endocrine pathology", PhD Thesis, Medical Domain, Cluj-Napoca 2005.

[6] D. C. Bernard Jensen, "The Science and Practice of Iridology" Volume. 1 Hardcover, May. 2005.

[7] S. Amerifar, A.T. Targhi and M.M. Dehshibi, "Iris the picture of health: Towards medical diagnosis of diseases based on iris pattern, In Proceedings of the 2015 Tenth International Conference on Digital Information Management (ICDIM), Jeju, Korea, Oct. 2015, 120-123. 45.

[8] S. Muzamil, T. Hussain, A. Haider, U. Waraich, U. Ashiq and E. Ayguadé, "An Intelligent Iris Based Chronic Kidney Identification System, *Symmetry*, Dec. 2020, 12, 2066.

[9] S. E Hussein, O.A. Hassan and M. H. Granat, "Control. Assessment of the potential iridology for diagnosing kidney disease using wavelet analysis and neural networks, *Biomedical Signal Processing and Control*, Volume. 8 Issue 6 Nov. 2013, 534-541.

[10] S. A. P. Leonardus, R. Rizal Isnanto, A. Triwiyatno and V. A. Gunawan, "Heart Disease Detection using Iridology with Principal Component Analysis (PCA) and Backpropagation Neural Network, The 7th Engineering International Conference, Engineering International Conference on Education, Concept and Application on Green Technology EIC 2018, 257-264.

[11] Benedictor.A. N., "Iris features-based heart disease diagnosis by computer vision, Conference: Ninth International Conference on Digital Image Processing (ICDIP 2017). Proc. of SPIE Vol. 10420 104203X-2

[12] D. H. Hareva, Samuel Lukas, Natanael Oktavian Suharta. "The Smart Device for Healthcare Service: Iris diagnosis application, Conference Paper, Computer Science, Nov. 2013.

[13] R.A.N.P Herlambang, R.R.Isnanto and A.Z.Ajub, "Application of liver disease detection using iridology with back-propagation neural network, In Proceedings of the 2015 2nd International Conference on Information Technology, Computer, and Electrical Engineering (ICITACEE), Semarang, Indonesia, Oct. 2015, 123-127.

[14] J.D. Miranda and S.A. Salinas, "Computational Measuring Approach for the Identification of Probable Intestinal System Pathologies through the Human Iris Parameters. In Proceedings of the 2019 XXII Symposium on

- Image, Signal Processing and Artificial Vision (STSIVA), Bucaramanga, Colombia, April. 2019, 1–5.
- [15] V. E. Carrera and M. Jennifer, "Computer Aided Diagnosis of Gastrointestinal Diseases Based on Iridology, Conference Paper, CITT 2018, CCIS 895, Nov. 2019. 531–541.
- [16] T. Anna, H. Suwastio and R. Damayanti, "Lung disorders detection based on irises image using computational intelligent art, TEKTRIKA-Jurnal Penelitian dan Pengembangan Telekomunikasi, Kendali, Komputer, Elektrik, dan Elektronika 2003, 8. [CrossRef].
- [17] T. Hussain, A. Haider, A.M. Muhammad, A. Agha, B. Khan, F. Rashid, M.S. Raza, M. Din, M. Khan and S. Ullah, " An Iris based Lungs Pre-diagnostic System, In Proceedings of the 2019 2nd International Conference on Computing, Oct. 2019.
- [18] A. D. Wibawa and H. P. Mauridhi, "Early Detection on the Condition of Pancreas Organ as the Cause of Diabetes Mellitus by Real Time Iris Image Processing, IEEE Asia Pacific Conference on Circuits and Systems, APCCAS 2006, Dec. 2006, 4-7.
- [19] P. D. Lesmana, I. P. D., Purnama, I. K. E and M. H. Purnomo, "Abnormal condition detection of pancreatic Beta-cells as the cause of Diabetes Mellitus based on iris image, 2nd International Conference on Instrumentation, Communications, Information Technology and Biomedical Engineering, Oct. 2011.
- [20] G. Burak Kırışat and C. Kurnaz, "Detection of high-level cholesterol in blood with iris analysis, 20th National Biomedical Engineering Meeting (BIYOMUT), Nov. 2016.
- [21] P. Knipschild. "Looking for gall bladder disease in the patient's iris, British Medical Journal, vol. 297 Dec. 1988. 1578-1581.

Cite this article as: Rana Cheikh Ousman, Mouhamad Tamer Zakor, Performance of F.S.G. Iridology in detecting all diseases, vitamins, and trace mineral in human body within one minute, *International journal of research in engineering and innovation (IJREI)*, vol 5, issue 6 (2021), 356-370. <https://doi.org/10.36037/IJREI.2021.5604>